Climate Dynamics (2006) 26: 713–728
DOI 10.1007/s00382-006-0110-3

Steven J. Lambert · John C. Fyfe

# Changes in winter cyclone frequencies and strengths simulated in enhanced greenhouse warming experiments: results from the models participating in the IPCC diagnostic exercise

Received: 20 May 2005 / Accepted: 5 December 2005 / Published online: 24 January 2006


**Abstract** The effect of enhanced greenhouse warming on the behaviour of mid-latitude cyclones is examined for changes in the total number of cyclone events and for changes in the number of intense events using the daily averaged mean sea level pressure simulated by coupled climate models participating in the IPCC AR4 (Fourth Assessment Report) diagnostic exercise. Results are presented for a set of scenarios which were produced using a wide range of increasing levels of greenhouse gases. For the enhanced greenhouse warming experiments, the models simulated a reduction in the total number of events and an increase in the number of intense events. This is a robust result, which essentially all the models exhibit. Comparison of the results for each of the scenarios shows that the magnitude of the changes in the number of simulated events increases with increasing levels greenhouse gas forcing used in the scenarios. Even though the numbers of events change, there is no apparent change seen in the geographical distribution of the events, i.e. there is no obvious change in the positions of the storm tracks seen on hemispheric charts. This was also evident in the results for the filtered variance of the meridional wind which was used as a proxy for cyclone activity. In spite of this, it is possible that small shifts in the storm tracks, which are difficult to resolve with the relatively coarse grid used for analysis, could occur.

## 1 Introduction

Cyclones are an important feature of the observed weather and climate. Regions influenced by migratory cyclones not only experience frequent cloudiness and precipitation but also experience a relatively high degree of variability caused by the alternation between cyclonic and anticyclonic regimes. In addition, since many extreme events in nature are related to cyclones, it is important to understand how their behaviour might change with global warming.

Simulations made using general circulation models (GCM) suggest that enhanced greenhouse warming will result in a general cooling of the stratosphere and a warming of the lower troposphere. The tropospheric warming is expected to be greater in polar regions than in the tropics, greater over continents than oceans, and greater in winter than in summer. This differential warming results in a reduction of the pole to equator thickness gradient in the lower troposphere. Diagnostic studies, e.g., those based on the Sutcliffe–Petterssen development equation (Sutcliffe and Forsdyke 1950; Petterssen 1956) show the relevance of the thickness field on the development of cyclones. The reduced thicknesses expected with warming should lead to fewer extra-tropical cyclones, especially in winter. However, since there is also an expected increase in surface and near surface temperatures this could lead to increased evaporation and elevated levels of atmospheric humidity. This favours increased precipitation in cyclones and the increased release of latent heat would result in increased development of cyclones. Clearly, these two processes tend to oppose each other and it is not clear how the two processes might contribute to changes in the cyclone climatology in a warmer world.

Since GCMs simulate the evolution of the day-to-day weather, they are an attractive tool to examine the influence of global warming on cyclone behaviour. Similar numerical models, even those which were unsophisticated by current day standards, have been used for decades in day-to-day weather forecasting. Such models have been very successful in simulating the structure and temporal evolution of mid-latitude cyclones. Based on this, it could be argued that climate models are well suited to provide reliable projections of future frequencies and strengths of mid-latitude cyclones.

S. J. Lambert (✉) · J. C. Fyfe
Canadian Centre for Climate Modelling and Analysis
Meteorological Service of Canada, University of Victoria,
PO Box 1700, Victoria, BC V8W 2Y2, Canada
E-mail: Steven.Lambert@ec.gc.ca

The effect of enhanced greenhouse warming on cyclone strengths and frequencies was first reported in Lambert (1995). This study examined changes in the cyclone climatology for an *equilibrium* double $CO_2$ simulation using an early version of the Canadian Centre for Climate Modelling and Analysis (CCCma) model (Boer et al. 1992). The results showed a decrease in the total numbers of cyclone events during winter in both the Northern and the Southern Hemispheres. Although the total number of cyclone events decreased with enhanced greenhouse warming, the number of intense cyclone events increased. There was, however, no noticeable change in the geographical positions of the storm tracks. A subsequent study of *transient* simulations by two versions of the CCCma model (Lambert 2004), showed the same result, i.e., the total number of cyclone events decreased and the number of intense events increased with global warming.

It would increase confidence in model projections if the behaviour of cyclones seen in the CCCma model were exhibited by a range of models. To this end, an IPCC (Intergovernmental Panel on Climate Change) diagnostic subproject was undertaken to examine the effect of enhanced warming on the behaviour of cyclones in a wide variety of coupled models. Modelling groups were requested to undertake a comprehensive series of experiments and to send their data to the Program for Climate Model Diagnosis and Intercomparison (PCMDI) where they were made available for analysis. The data obtained from this site are analyzed and the results are reported in subsequent sections.

## 2 Data and analysis

The effect of enhanced greenhouse warming on cyclone frequencies and strengths is examined using the daily averaged mean sea level pressure (MSLP) simulated by coupled models participating in the IPCC AR4 (Fourth Assessment Report) diagnostic exercise. The modelling groups provided data from a wide range of scenarios. Of primary interest are the data from the four scenarios initiated from climate of the twentieth century simulations. They are the 'committed' climate change experiment and the SRES B1, SRESA1B, SRESA2 experiments. The models used in this analysis and the data available are listed in Table 1.

For completeness, two other experiments which are initialized from the pre-industrial control simulations: namely, the 1% increase in carbon dioxide to doubling and the 1% increase in carbon dioxide to quadrupling are also examined. The models used in these analyses and the data available are given in Table 2.

The model data were received on a variety of grids which were interpolated to northern and southern polar stereographic grids with a grid spacing of 381 km at 60°N and 60°S. For the models with data on Gaussian grids, the data were transformed to arrays of spectral coefficients with a triangular truncation at 40 waves. The spectral data were then synthesized on the polar stereographic grids. For those models with data on latitude–longitude grids, the data were first interpolated to Gaussian grids with roughly the same number of latitudes and longitudes as the latitude–longitude grid. From this point, the conversion to polar stereographic grids followed the procedure used for models with their data on Gaussian grids. Some of the latitude–longitude grids did not have sufficient resolution to support a spectral representation at 40 waves. For these models, a triangular truncation of 32 waves was used.

In order to study the behaviour of cyclones in many experiments from a group of models an objective procedure must be used and a wide variety of such procedures have been developed. The simplest of these is described in Lambert (1995) in which the sole criterion for the identification of a cyclone event is the occurrence of an MSLP value which is lower than each of the four surrounding grid points. The advantages of this method are that it requires only the MSLP field, it is conceptually straight forward and it will provide the geographical positions and central pressures of cyclones. The major disadvantage of this procedure is that it will identify features which are not mid-latitude cyclones such as thermal lows and lows produced when extrapolating under regions of high terrain. The above counting procedure was used by Lambert et al. (2002) to extract the 10-year cyclone event climatologies from a collection of GCMs participating in AMIP and from two observation-based datasets. Comparison of the latter two to long term climatologies, e.g., Petterssen (1956), showed that, despite its simplicity, the technique produced climatologies which were in agreement with those produced manually from a long series of analyzed charts.

Using the data on the polar stereographic grids, the cyclone event frequencies poleward of 30° were extracted using the daily averaged MSLP data from the various models and experiments. Most of the scenario data were available as 20-year time series and the pre-industrial control run and the climate of the twentieth century runs as 40-year time series. The number of cyclone events over these periods was accumulated at each grid point. The frequencies were computed for 120-day winter seasons beginning on 15 November for the Northern Hemisphere and 120-day seasons beginning on 15 May for the Southern Hemisphere.

Previous work indicated that intense cyclones will increase with enhanced warming and the total number of events will decrease. In order to address this in the IPCC models, the number of intense events and the total number of events were enumerated separately. In the Northern Hemisphere, an intense event is defined as the occurrence of a pressure lower than 970 mb at the central grid point. The number of deep cyclones varies considerably from model to model with the result that the constant threshold stated above will identify a higher fraction of events as intense in models which produce a relatively large number of deep cyclones. An alternative to using a constant threshold is to define intense events

**Table 1** Data available for analysis of the experiments initialized using the year 2000 values from climate of the twentieth century (20c3m) simulations, i.e.,'committed' climate change, the SRES B1, SRES A1B, and SRES A2

| Model | Grid | 20c3m | Commit | sresb1 | sresa1b | seresa2 |
|---|---|---|---|---|---|---|
| cccma_t47 | http://www.cccma.bc.ec.gc.ca/models/cgcm3.shtml | | | | | |
| | Gaussian 96×48 | 1961–2000 | 2046–2065 | 2046–2065 | 2046–2065 | 2046–2065 |
| | | | 2081–2100 | 2081–2100 | 2081–2100 | 2081–2100 |
| | | | | 2181–2200 | | |
| | | | | 2281–2300 | | |
| cnrm | D. Salas-Mélia et al. (submitted) | | | | | |
| | Gaussian 128×64 | 1961–2000 | 2046–2065 | 2046–2065 | 2046–2065 | 2046–2065 |
| | | | 2081–2100 | 2081–2100 | 2081–2100 | 2081–2100 |
| | | | | 2181–2200 | 2181–2200 | |
| | | | | 2281–2300 | 2281–2300 | |
| gfdl_2.0 | Delworth et al. (2005) | | | | | |
| | Gnanadesikan et al. (2005) | | | | | |
| | Latitude/longitude 144×90 | 1961–2000 | 2046–2065 | 2046–2065 | 2046–2065 | 2046–2081 |
| | | | 2081–2100 | 2081–2100 | 2081–2100 | 2081–2100 |
| | | | | 2181–2200 | 2181–2200 | |
| | | | | 2281–2300 | 2281–2300 | |
| gfdl_2.1 | Delworth et al. (2005) | | | | | |
| | Gnanadesikan et al. (2005) | | | | | |
| | Latitude/longitude 144×90 | 1961–2000 | 2046–2065 | 2046–2065 | 2046–2065 | 2046–2065 |
| | | | 2081–2100 | 2081–2100 | 2081–2100 | 2081–2100 |
| | | | | 2181–2200 | 2181–2200 | |
| | | | | 2281–2300 | 2281–2300 | |
| giss_aom | Russell et al. (1995) http://www.aom.giss.nasa.gov | | | | | |
| | Latitude/longitude 90×60 | 1961–2000 | | 2046–2065 | 2046–2065 | |
| | | | | 2081–2100 | 2081–2100 | |
| giss_e_h | Schmidt et al. (2005) | | | | | |
| | Bleck (2002) | | | | | |
| | Latitude/longitude 72×46 | 1961–2000 | | | | |
| giss_e_r | Schmidt et al. (2005) | | | | | |
| | Russell et al. (2000) | | | | | |
| | Latitude/longitude 72×46 | 1961–2000 | 2046–2065 | 2046–2065 | 2046–2065 | 2046–2065 |
| | | | 2081–2100 | 2081–2100 | 2081–2100 | 2081–2100 |
| | | | | 2181–2200 | 2181–2200 | |
| | | | | 2281–2300 | 2281–2300 | |
| inm | Diansky and Volodin (2002) | | | | | |
| | Latitude/longitude 72×45 | 1961–2000 | 2046–2065 | 2046–2065 | 2046–2065 | 2046–2065 |
| | | | 2081–2100 | 2081–2100 | 2081–2100 | 2081–2100 |
| | | | | 2146–2165 | 2146–2165 | 2146–2165 |
| | | | | 2181–2200 | 2181–2200 | 2181–2200 |
| ipsl | http://www.dods.ipsl.jussieu.fr/omamce/IPSLCM4/DocIPSLCM4/FILES/DocIPSLCM4.pdf | | | | | |
| | Latitude/longitude 96×72 | 1961–2000 | 2046–2065 | 2046–2065 | 2046–2065 | 2046–2065 |
| | | | 2081–2100 | 2081–2100 | 2081–2100 | 2081–2100 |
| miroc_med | http://www.ccsr.u-tokyo.ac.jp/kyosei/hasumi/MIROC/tech-repo.pdf | | | | | |
| | Gaussian 128×64 | 1961–2000 | 2046–2065 | 2046–2065 | 2046–2065 | 2046–2065 |
| | | | 2081–2100 | 2081–2100 | 2081–2100 | 2081–2100 |
| | | | | 2181–2200 | 2181–2200 | |
| | | | | 2281–2300 | 2281–2300 | |
| miroc_hi | http://www.ccsr.u-tokyo.ac.jp/kyosei/hasumi/MIROC/tech-repo.pdf | | | | | |
| | Gaussian 320×160 | 1961–2000 | | 2046–2065 | 2046–2065 | |
| | | | | 2081–2100 | 2081–2100 | |
| echam5_mpi | Roechner et al. (2003) | | | | | |
| | Marsland et al. (2003) | | | | | |
| | Gaussian 192×96 | 1961–2000 | 2046–2081 | 2046–2065 | 2046–2065 | 2046–2065 |
| | | | 2081–2100 | 2081–2100 | 2081–2100 | 2081–2100 |
| | | | | 2181–2200 | 2181–2200 | |
| | | | | | 2281–2300 | |
| mri | Yukimoto et al. (2001) | | | | | |
| | Gaussian 128×64 | 1961–2000 | 2046–2065 | 2046–2065 | 2046–2065 | 2046–2065 |
| | | | 2081–2100 | 2081–2100 | 2081–2100 | 2081–2100 |
| | | | | 2181–2200 | 2181–2200 | |
| | | | | 2281–2300 | 2281–2300 | |

**Table 1** (Contd.)

| Model | Grid | 20c3m | Commit | sresb1 | sresa1b | seresa2 |
|---|---|---|---|---|---|---|
| ncar_pcm | Washington et al. (2000) | | | | | |
| | Gaussian 128×64 | (1) 1890–1999 | (2) 2000–2069 | (1) 2200–2299 | (2) 2100–2199 | (1) 2000–2099 |
| | | (2) 1890–1999 | (3) 2000–2099 | (2) 2000–2099 | | |
| | | (3) 1890–1999 | | (3) 2000–2099 | | |
| | | (4) 1890–1999 | | (4) 2100–2199 | | |
| ncar_ccsm | W. D. Collins et al. (submitted) | | | | | |
| | Gaussian 256×128 | (1) 1870–1999 | (1) 2000–2099 | (2) 2000–2099 | (2) 2000–2099 | |
| | | (3) 1870–1999 | (2) 2000–2099 | (6) 2000–2099 | (3) 2000–2099 | |
| | | (6) 1870–1999 | (3) 2000–2099 | (7) 2000–2099 | (5) 2000–2199 | |
| | | | (4) 2000–2099 | (8) 2000–2099 | (7) 2000–2349 | |
| | | | (6) 2000–2049 | | | |

The table lists the models used and their references, the grids on which the data were provided, and the time slices for which the data were available. Multiple realizations were received from two models and these are identified by the run number in parentheses to the left of the time slices

as a constant fraction of the total number of events. For this study we have opted, where possible, to use a constant threshold. Sensitivity tests were run on the choice of the threshold and it was found that qualitatively results are not particularly sensitive to the value used. In the Southern Hemisphere, higher numbers of intense cyclones are simulated than in the Northern Hemisphere and a lower threshold of 960 mb is used to define intense events. One of the models, *NCAR_CCSM*, simulated a very large number of intense events with some of the lows exhibiting depths approaching 900 mb. Using the above thresholds for this model resulted in an inordinate number of intense events and this necessitated the use of thresholds 10 mb lower than that of the others for this model. Given the large variability in the number of intense events simulated by the models, an intense event is not necessarily an extreme event.

**Table 2** Data available for the experiments initialized using the pre-industrial control simulation (picntrl); the 1pctto2x and the 1pctto4x experiments. The table lists the models and the time slices available for each

| Model | picntrl | 1pctto2x | 1pctto4x |
|---|---|---|---|
| cccma_t47 | 1961–2000 | 1910–1929 | 1980–1999 |
| | | 2050–2069 | 2120–2139 |
| cnrm | 1961–2000 | 1910–1929 | 1990–2009 |
| | | 2061–2080 | |
| gfdl_2.0 | 0101–0140 | 0061–0080 | 0131–0150 |
| | | 0201–0220 | 0271–0290 |
| gfdl_2.1 | 0141–0180 | 0061–0080 | 0131–0150 |
| | | 0201–0220 | 0271–0290 |
| giss_aom | 1961–2000 | | |
| | 2046–2065 | | |
| | 2081–2100 | | |
| giss_e_h | (1) 2120–2159 | | |
| giss_e_r | 1987–2026 | 2101–2120 | 2171–2190 |
| inm | 1961–2000 | 1931–1950 | 2001–2020 |
| | | 2071–2090 | 2141–2160 |
| ipsl | 1961–2000 | 1921–1940 | 1991–2010 |
| | | 2061–2080 | |
| miroc_med | 2411–2450 | 0061–0080 | 0131–0150 |
| | | 0201–220 | 0271–0290 |
| miroc_hi | 0060–0099 | 0060–0080 | |
| echam5_mpi | | 1921–1940 | 1991–2010 |
| | | 2061–2080 | 2131–2150 |
| mri | 1961–2000 | 2001–2020 | 2071–2090 |
| ncar-pcm | (1) 0451–1199 | | |
| ncar-ccsm | (1) 0280–0509 | | |
| | (2) 0430–0799 | | |

## 3 Results

All modelling groups produced a 40-year simulation of the late twentieth century climate. There are observations available for this period and this provides an opportunity to evaluate the simulations of the current cyclone event climatology. Table 3 gives the total number of cyclone events and the number of intense events simulated by each model and corresponding statistics computed from the ERA40 reanalyses. The results for the total number of events in both hemispheres indicate that, as a group, the models tend to underestimate slightly the number of observed events. For the intense events, there is considerable inter-model variability. In general, compared to the Northern Hemisphere, there are more intense events simulated and observed in the Southern Hemisphere in spite of the fact that the intense event threshold is 10 mb lower. One might be concerned that the wide range in the number of simulated intense events would cause problems for the analysis. It will be seen a posteriori that, qualitatively, the models exhibit a similar response to enhanced warming regardless of the absolute numbers of intense events which are simulated.

It should be bourne in mind that the central pressure of a cyclone results from the baroclinic processes producing it and the "background" pressure field in which the cyclone is imbedded. Consequently, a decrease in central pressure could also reflect a decrease in the background pressure field as well as a decrease in cyclone depth. No attempt was made to separate these two contributions.

A set of climate change experiments were undertaken by most of the modelling groups. Figure 1 shows the

**Table 3** The number of total and intense events simulated by the models for the period 1961–2000 from the climate of the twentieth century simulations and the number observed events extracted from the ERA40 reanalyses for both the Northern and the Southern Hemispheres

| 1961–2000 | Northern Hemisphere | | Southern Hemisphere | |
|---|---|---|---|---|
| Model | Total | Intense | Total | Intense |
| cccma_t47 | 99,708 | 2,374 | 78,850 | 7,009 |
| cnrm | 68,887 | 399 | 57,995 | 147 |
| gfdl_2.0 | 88,013 | 2,294 | 74,027 | 5,737 |
| gfdl_2.1 | 89,246 | 1,986 | 70,736 | 6,543 |
| giss_aom | 75,700 | 732 | 64,828 | 522 |
| giss_e_r | 96,000 | 873 | 82,365 | 1,245 |
| giss_e_h | 92,256 | 1,791 | 82,312 | 2,054 |
| inm | 61,482 | 2,175 | 53,166 | 4,598 |
| ipsl | 8,1271 | 3,838 | 67,669 | 2,773 |
| miroc_hires | 89,905 | 3,977 | 82,350 | 3,672 |
| miroc_medres | 91,681 | 3,278 | 92,176 | 8,272 |
| echam5_mpi | 94,318 | 1,959 | 76,405 | 6,956 |
| mri | 89,180 | 1,495 | 81,835 | 2,269 |
| ccsm_run1 | 81,393 | 2,275 | 66,563 | 7,753 |
| ccsm_run3 | 80,931 | 2,449 | 67,067 | 7,615 |
| ccsm_run6 | 82,371 | 2,244 | 66,604 | 7,518 |
| pcm_run1 | 88,459 | 2,640 | 72,463 | 11,897 |
| pcm_run2 | 87,556 | 2,694 | 71,404 | 12,362 |
| pcm_run3 | 88,699 | 2,566 | 71,576 | 12,284 |
| pcm_run4 | 88,350 | 2,532 | 71,148 | 12,615 |
| model mean | 85,770 | 2,229 | 72,577 | 6,192 |
| era40 | 93,734 | 2,118 | 74,074 | 4,767 |

For the Northern Hemisphere intense lows have a central pressure less than 970 mb and for the Southern Hemisphere intense lows have a central pressure less than 960 mb

$CO_2$ abundances as a function of time used in these experiments (Houghton et al. 2001). In the following sections, the results of the analysis of the total number of cyclone events and the number of intense events are presented.

### 3.1 "Committed" climate change experiment

As indicated in Fig. 1, in this scenario, the models were integrated to the year 2100 holding the level of greenhouse gases constant at year 2000 levels. Under such a scenario, climate change results from the ocean, with its long time scales, attempting to come into equilibrium with the year 2000 forcing. In general, the modelling groups provided two 20-year periods of simulated data, from 2046 to 2065 and from 2081 to 2100.

Data from 12 models were available for analysis. Figure 2 displays the results as a departure of the number of simulated events from the climate of the twentieth century simulation for the two periods. The large black dots represent the mean over the 12 models. Figure 2a, c gives the results for the total number of events for the Northern and the Southern Hemispheres, respectively. All models simulate a reduction in the number of events over the 1961–2000 to 2046–2065 period. Between 2046–2065 and 2081–2100, the individual models exhibit a variety of behaviour but the mean is nearly constant. Figure 2b, d gives the corresponding results for the intense events. There are far fewer intense events than total events which results in increased sampling variability. Over the period 1961–2000 to 2046–2065, the models simulate a general increase in the number of intense events and a less consistent behaviour between 2046–2065 and 2081–2100. The model mean displays an increase over the first period followed by a reduced increase over the second period.

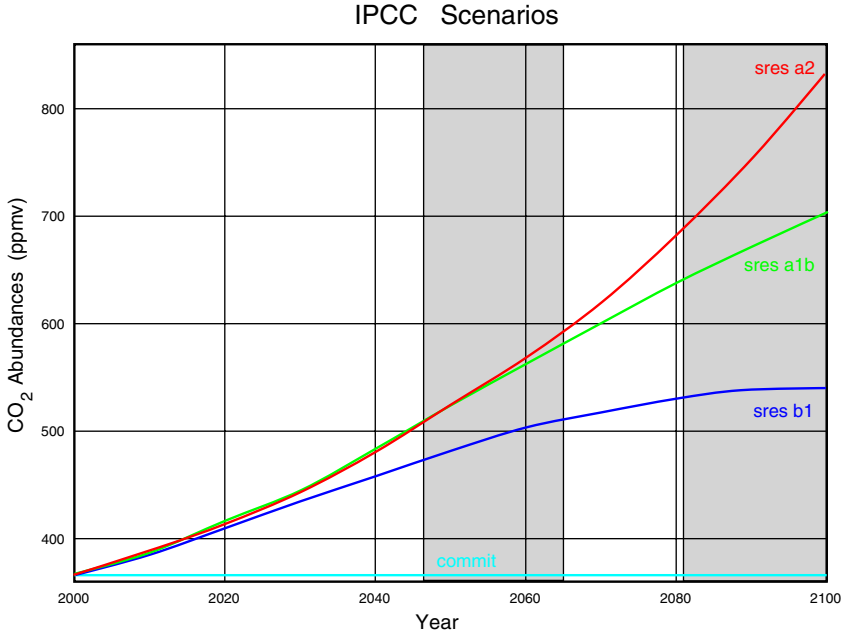


**Fig. 1** The changes in the levels of carbon dioxide used between 2000 and 2100 for the 'committed' climate change, the SRES B1, the SRES A1B, and the SRES A2 experiments

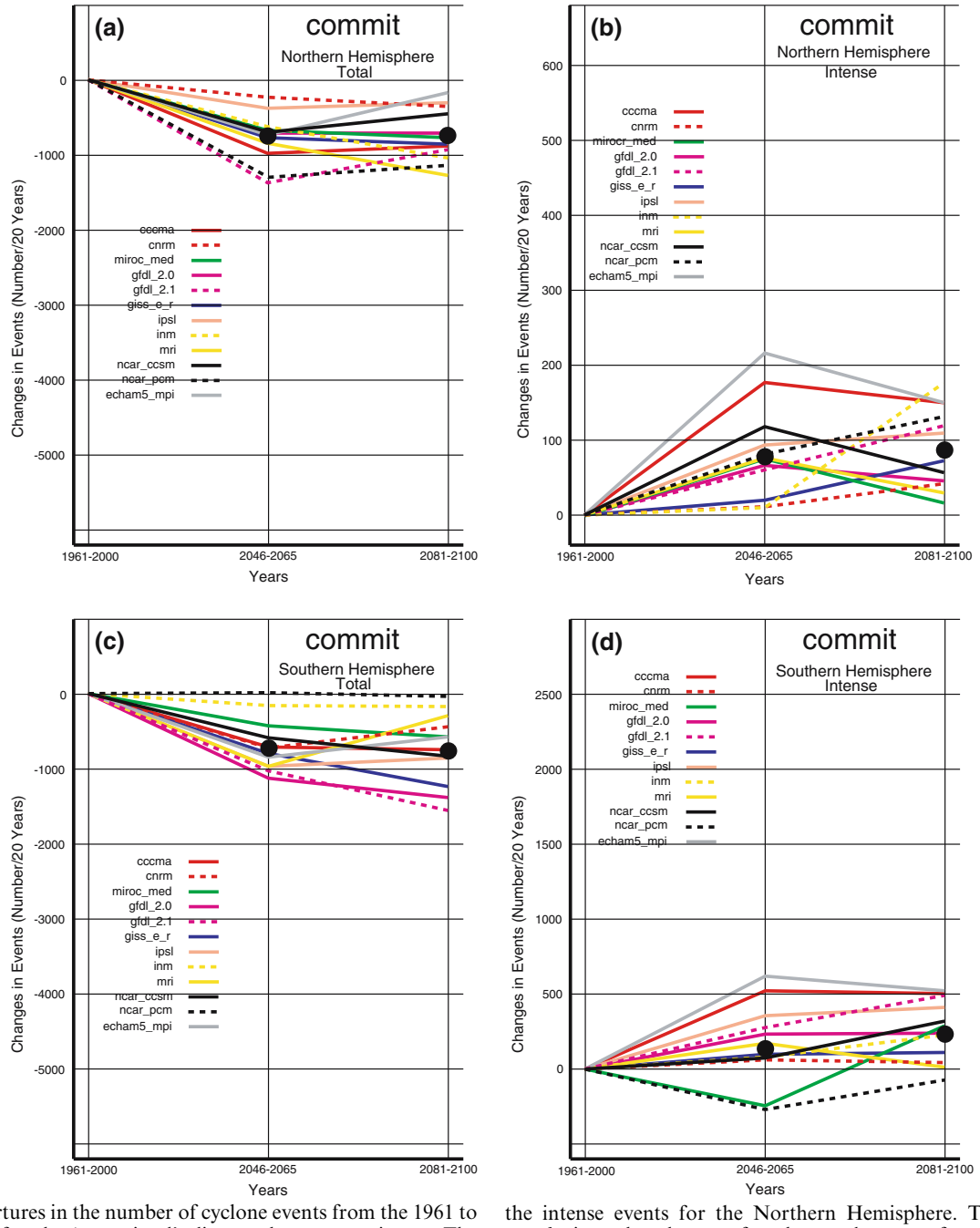


**Fig. 2** Departures in the number of cyclone events from the 1961 to 2000 period for the 'committed' climate change experiment. The *upper left panel* displays the changes in total events for the Northern Hemisphere, the *upper right panel* displays the change in the intense events for the Northern Hemisphere. The *lower left panel* gives the changes for the total events for the Southern Hemisphere and the *lower right panel* gives the Southern Hemisphere results for the intense events

## 3.2 The SRES B1 climate change scenario

In this scenario, the models were to be integrated to the year 2300 with the level of greenhouse gases increasing from the year 2000 levels to roughly 550 ppmv at 2100 and constant thereafter. In general, the modelling groups provided four 20-year periods of simulated data: from 2046 to 2065, 2081 to 2100, 2181–2200, and 2281–2300.

Only seven groups provided all four periods but data were available from 14 models for the first two periods. Figure 3 displays the results as a departure of the number of simulated events from the climate of the twentieth century simulation as a function of time. The large black dots represents the mean over the available models. Figure 3a, c gives the results for the total number of events for the Northern and the Southern Hemispheres, respectively.The results are similar to

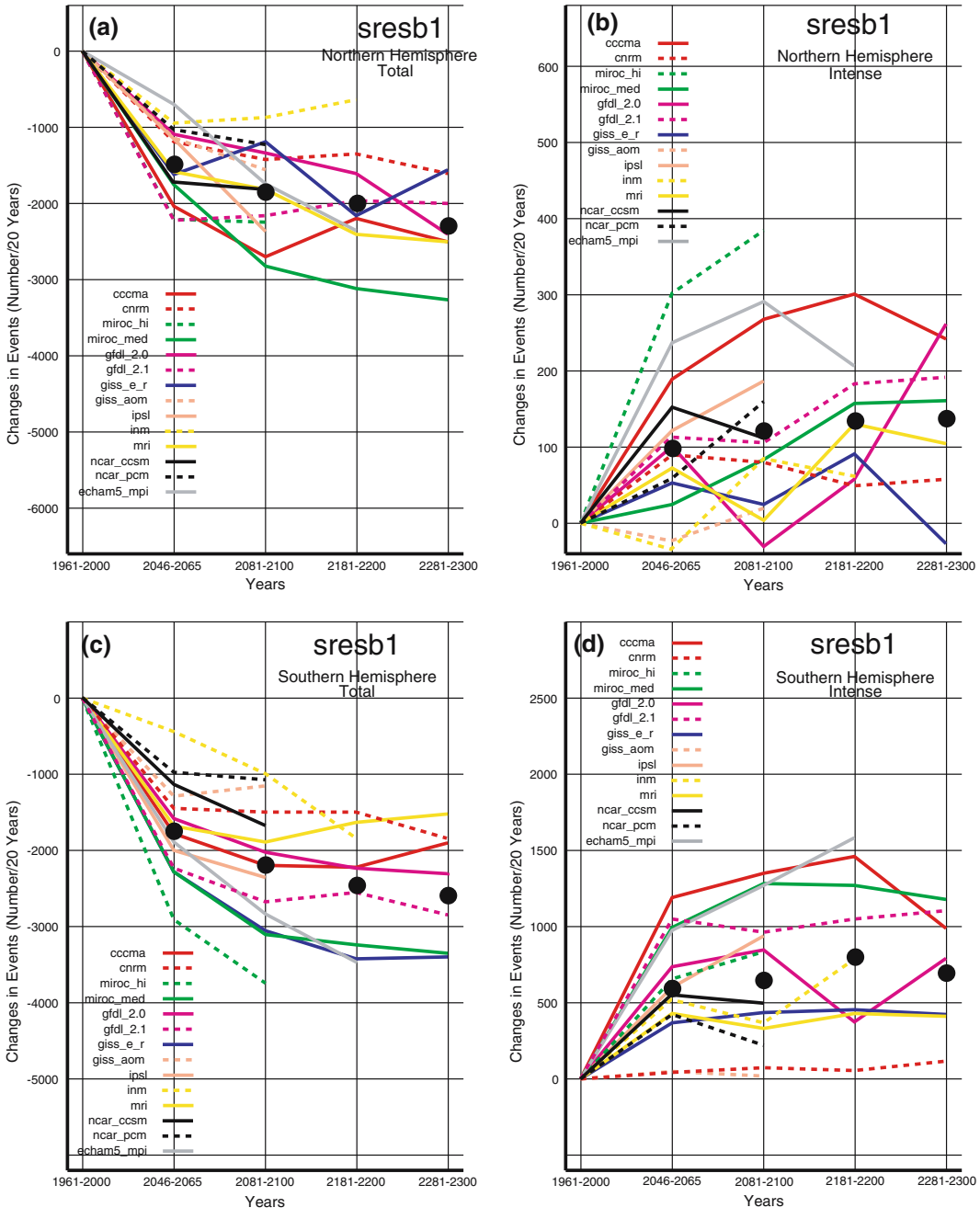


**Fig. 3** Same as Fig. 2 except for the SRES B1 scenario

those of the previous section in that there is a relatively large decrease over the period 1961–2000 and 2046–2065 and a noticeably smaller decrease thereafter. The reduction of the number of cyclone events in the mean is about 50% larger than that of the committed climate change experiments. Figure 3b, d gives the corresponding results for the intense events. These results are also qualitatively similar to those of the previous section. Over the period 1961–2000 to 2046–2065, the models simulate a general increase in the number of intense events and a less consistent behaviour between 2046–2065 and 2081–2100. The model means display an increase over the first period followed by a reduced increase or slight decrease over the remaining periods.

### 3.3 The SRES A1B climate change scenario

In this scenario, the models were to be integrated to the year 2300 with the level of greenhouse gases increasing from the year 2000 levels to roughly 720 ppmv at 2100 and constant thereafter. In general, the modelling groups

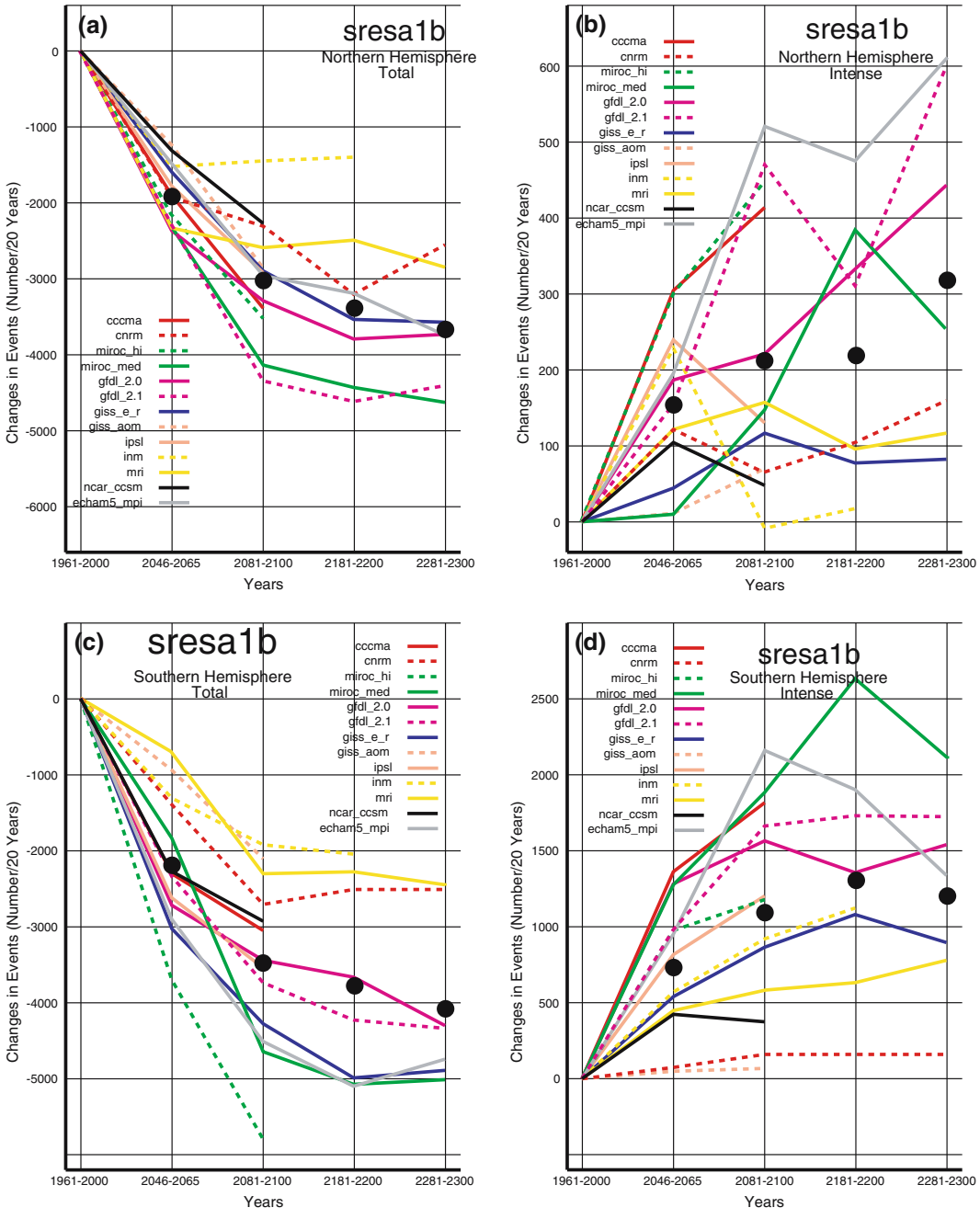


**Fig. 4** Same as Fig. 2 except for the SRES A1B scenario

provided four 20-year periods of simulated data: from 2046 to 2065, 2081 to 2100, 2181–2200, and 2281–2300.

Again, only seven groups provided all four periods but data were available from 13 models for the first two periods. Figure 4 displays the results as a departure of the number of simulated events from the climate of the twentieth century simulation as a function of time. The large black dots represents the mean over the available models. Figure 4a, c gives the results for the total number of events for the Northern and the Southern Hemispheres, respectively. This scenario shows a noticeable reduction in the number of cyclone events in both hemispheres. The rate of decrease of events is roughly constant until the 2081–2100 period and then tends to level off. This is in contrast to the previous results that showed the number of cyclone events becoming nearly constant after 2046–2065. The corresponding results for the intense events are given in Fig. 4b, d. These results show an increase in the number intense events which is larger than either of the previous two scenarios, reflecting the increased levels of $CO_2$ used in this scenario.

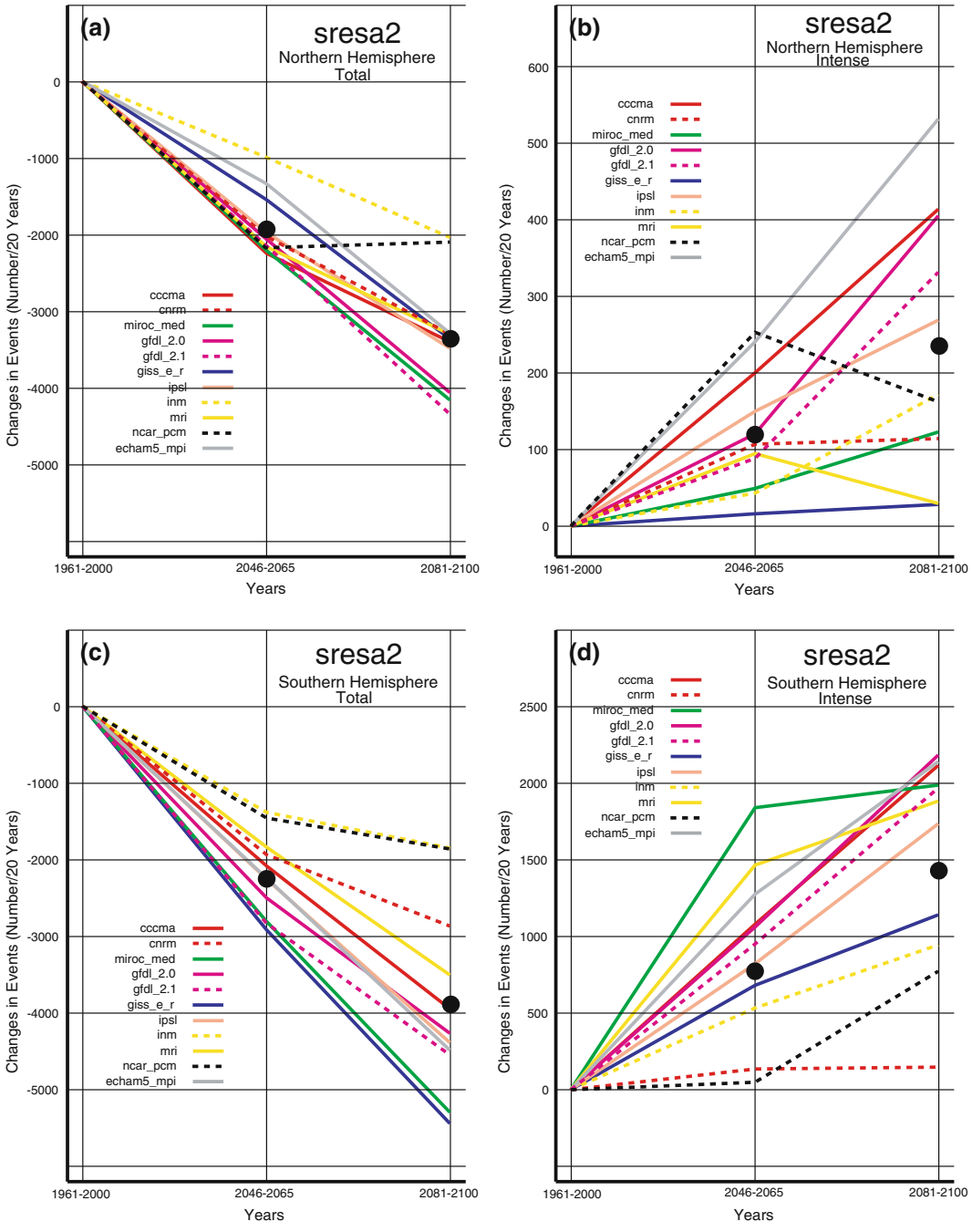


**Fig. 5** Same as Fig. 2 except for the SRES A2 scenario

### 3.4 The SRES A2 climate change scenario

In this scenario, the models were to be integrated to the year 2100 with the level of greenhouse gases increasing roughly exponentially from the year 2000 levels to roughly 840 ppmv at 2100. In general, the modelling groups provided two 20-year periods of simulated data: from 2046 to 2065 and 2081 to 2100.

Data were available from 11 groups. Figure 5 displays the results as a departure of the number of simulated events from the climate of the twentieth century simulation as a function of time. The large black dots represents the mean over the available models. Figure 5a, c gives the results for the total number of events for the Northern and the Southern Hemispheres, respectively. In both hemispheres, the results show a nearly linear decrease in the total number of events over the 100 years of integration, with the reduction during the 2081–2100 period being the largest of any of the previously discussed scenarios. The results for the intense

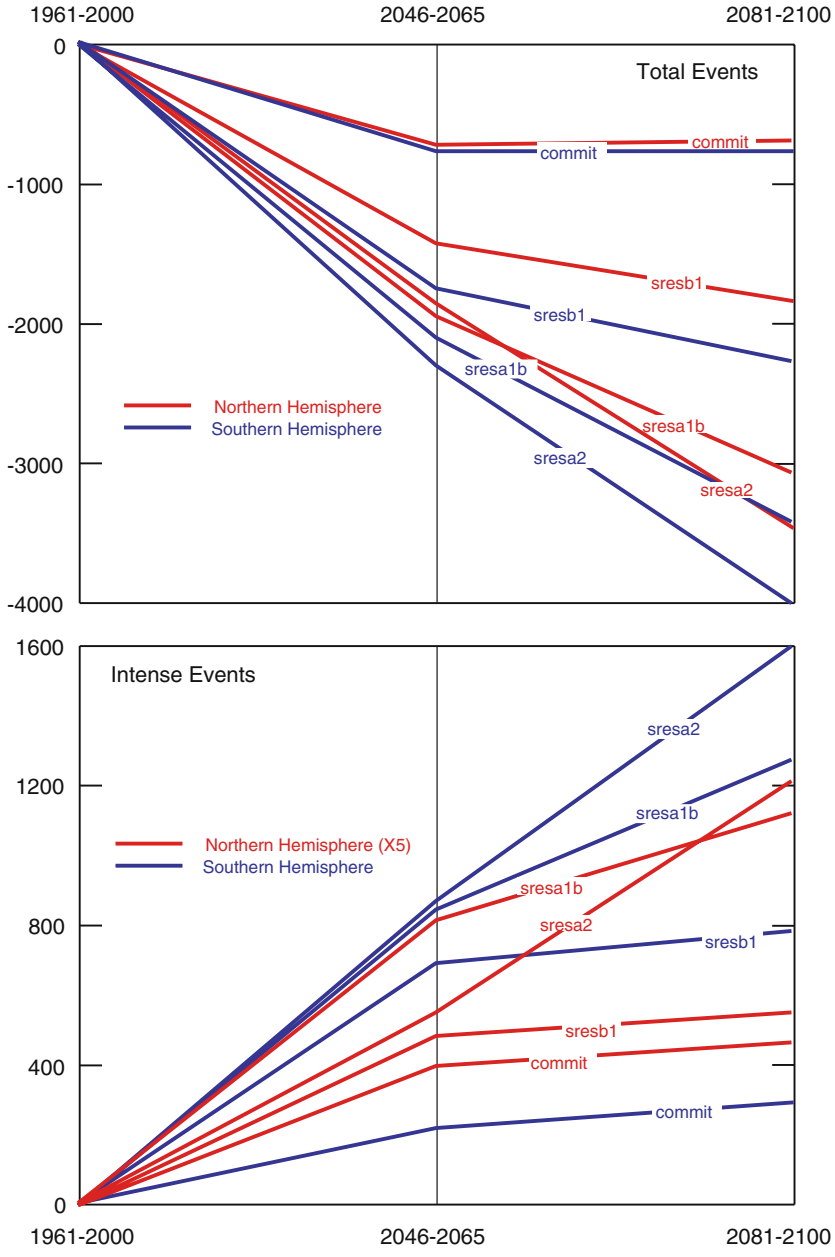


**Fig. 6** The model mean of the departures of events from 1961 to 2000 for the periods 2046–2065 and 2081–2100 for the 'committed' climate change, SRES B1, SRES A1B, and SRES A2 experiments. The *upper panel* displays the results for the total events with the Northern Hemisphere results in *red* and the Southern Hemisphere results in *blue*. The *lower panel* gives the corresponding results for the intense events. (Note that the Northern Hemisphere values have been scaled by a factor of 5 to aid the display.)

events are given in Fig. 5b, d. These results show an increase in the number intense events which is larger than any of the previous scenarios.

We now examine the change in the model means for each scenario in order to determine if there is a consistent relationship between changes in the cyclone events and the increases in the $CO_2$ levels used for each scenario. Model means are computed using only ten models for which data for both of the 2046–2065 and 2081–2100 periods and all four scenarios are available. For the intense events, the inter-model variability can be rather large, especially in the Northern Hemisphere, which could affect the representativeness of the means. These means will be slightly different from the means indicated as black dots on Figs. 2, 3, 4, and 5 since a different sample was used in computing them. Figure 6 displays the means for the total events and the intense events for both hemispheres and all four scenarios. These results clearly show that the magnitudes of the changes in the number of events vary directly with the levels of $CO_2$ used in the experiments.

### 3.5 The 1pctto2x and the 1pctto4x scenarios

Although it might be argued that the 1pctto2x and the 1pctto4x scenarios are less likely to occur under future climate change than the SRES scenarios, they do provide an additional opportunity to examine the model responses to relatively strong greenhouse forcing. The simulations for these two experiments were initiated from the pre-industrial control runs. For the 1pctto2x

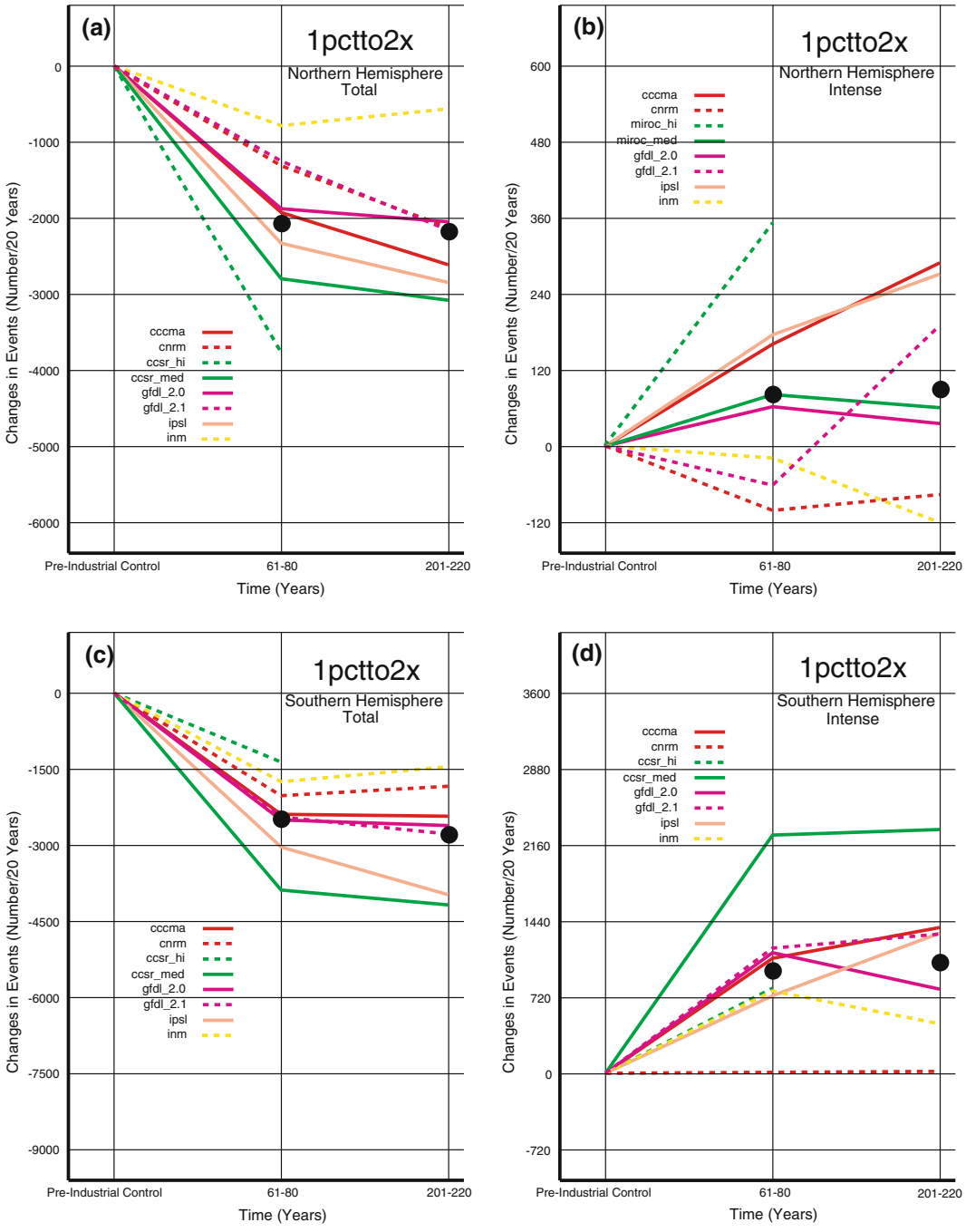


**Fig. 7** Same as Fig. 2 except for the 1pctto2x experiment

simulations, the models were integrated with the levels of $CO_2$ increasing at 1% per year until they were double those of the control run (about 70 years) and then held constant for an additional 150 years. The modelling groups provided outputs for the 20 years centred on the time of $CO_2$ doubling and the 20 years at the end of the simulation. The 1pctto4x simulations were performed in a similar manner except the levels of $CO_2$ were allowed to quadruple (about 140 years) before being held constant.

Figure 7a, c shows change in the total number of events for the $CO_2$ doubling experiments. All models exhibit a reduction in events during the period of doubling and a lesser reduction during the 150 year period when $CO_2$ levels were held fixed. Changes in the intense events are given in Fig. 7b, d. For the Northern Hemisphere, there is a considerable variability in the behaviour of the models. Most of the models exhibit an increase in the number of intense events, but in spite of the strong forcing, there are three for which the number of events decreased. Two

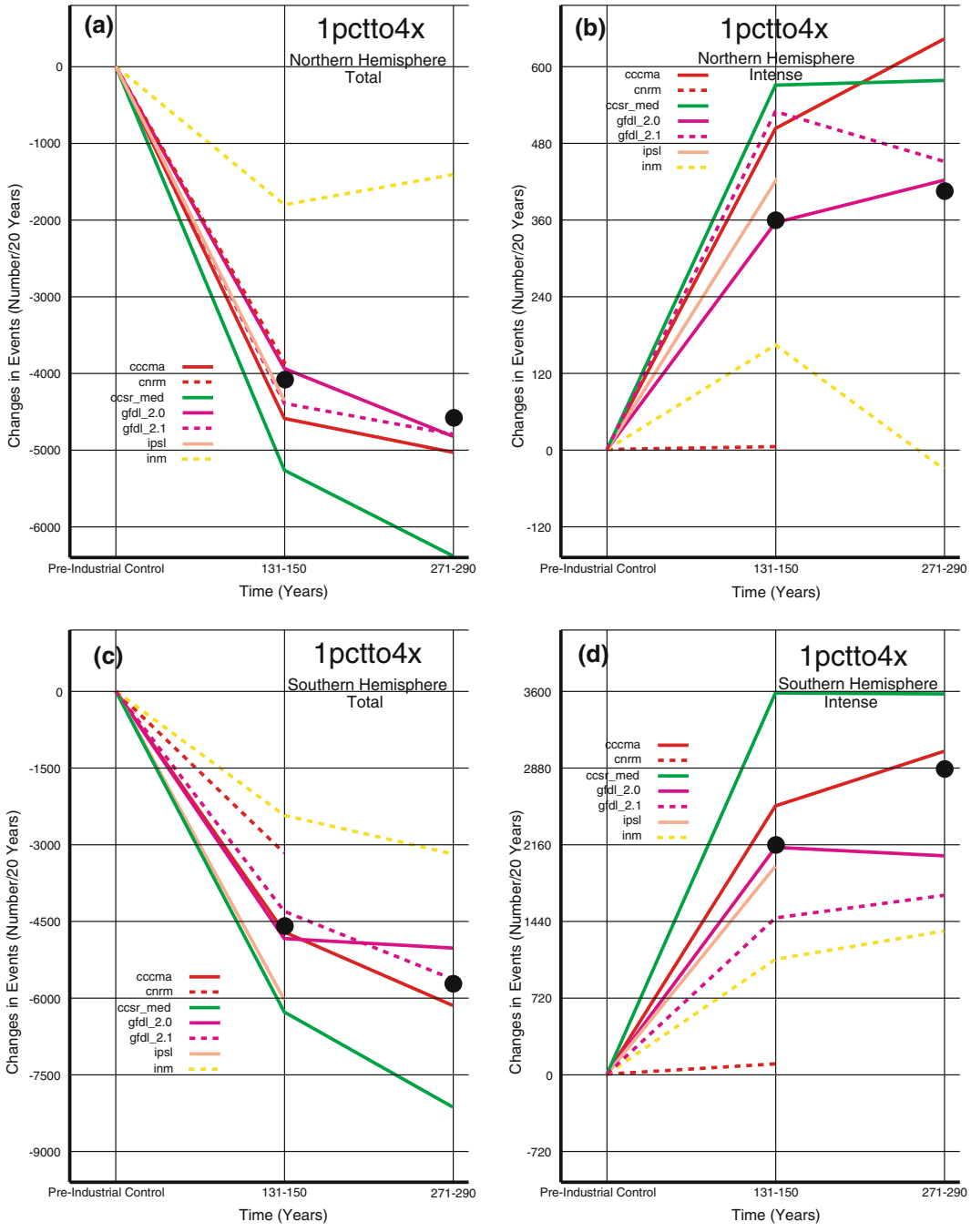


**Fig. 8** Same as Fig. 2 except for the 1pctto4x experiment

possible reasons for this are sampling problems or drift in the control simulation. The decrease shown by the *GFDL 2.1* model is likely the result of sampling since at the end of the simulation, the model simulates a noticeable increase in events. Given that the *CNRM* and the *INM* models exhibited increases in intense events in the SRES scenarios initialized from the twentieth century simulations, control run drift is a possible cause. Such a situation would arise if the segment of the control run that was made available at PCMDI was different from that used to initialize the 1pctto2x runs.

Figure 8 shows the corresponding results for the quadrupling of $CO_2$ case. As would be expected, the changes in both the total and intense events are larger than the $CO_2$ doubling case, general by about a factor of two.

### 3.6 The pre-industrial control and the twentieth century climate simulations

The levels of $CO_2$ used in the production of the twentieth century climate simulations are higher than those

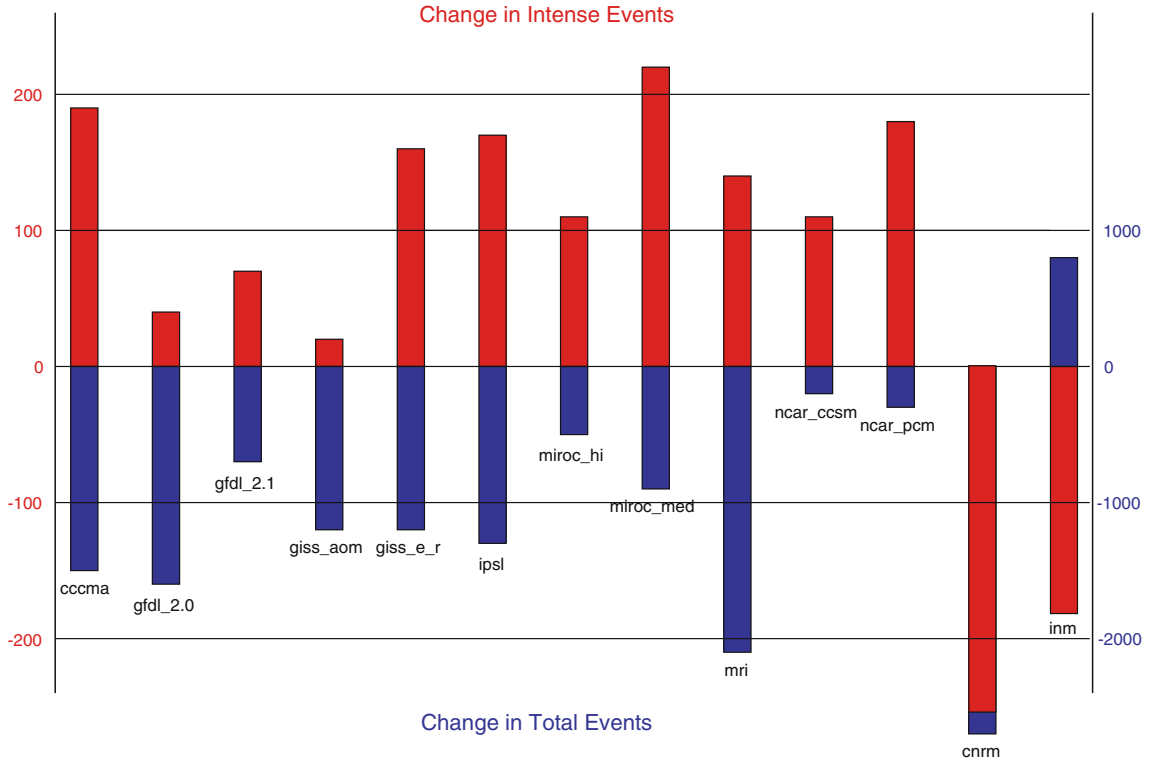


**Fig. 9** Differences in the number of events between the climate of the twentieth century and the pre-industrial control simulations for the Northern Hemisphere over a 40 year period. The *red bars* and the *red scale* refer to intense events and the *blue bars* and *blue scale* refer to the total events

used in the pre-industrial control simulations. Even though the change in forcing is relatively weak, it should nevertheless result in changes in the number of simulated cyclone events. Based on the previous results, one would expect the twentieth century simulation to produce more intense events and fewer total events than the pre-industrial control simulation. Figure 9 displays the departures from the control run. Most models exhibit the expected response as indicated by a red bar above a blue bar on the figure. The two models, *CNRM* and *INM*, which exhibited contrary behaviour in the 1pctto2x simulations, do not exhibit this behaviour and this could be interpreted as further evidence of drift in the control simulations.

The daily averaged MSLP field from the 45-year period spanned by the ERA40 reanalysis also exhibits a decreasing trend in the total number of events and an increasing trend in intense events, but these trends are not statistically significant.

### 3.7 Changes in the geographical positions of the storm tracks

The changes in the geographical distribution of the total cyclone events was examined for the climate change scenarios for each model. These results for both hemispheres indicate that there are no large changes in the position of the storm tracks seen on hemispheric charts. This is illustrated in Fig. 10, which compares the model mean climatology for the 1961–2000 period to that of 2081–2100 period of the SRES A1B experiments. (The data have been smoothed using a nine-point filter.) The results for both hemispheres show that there is no discernible spatial change in the storm tracks.

The shift in the cyclone tracks was also examined using an alternative measure of cyclone activity. The 500 mb meridional wind was filtered to retain periods between 2 and 6 days and the model means of its variance were computed for the period 1961–2000 from the climate of the twentieth century simulations and for the 2081–2100 period from the SRES A1B scenarios. The results are shown in Fig. 11. If the filtered variance patterns can be used as proxies for storm tracks then this result also shows that there is no large shift in the storm tracks with global warming.

Since a relatively coarse grid (~400 km) was used in the analysis, it is likely that the models do indeed predict small, difficult to resolve changes, in the positions of the storm tracks.

It was stated in Sect. 1 that one might expect a reduction in the total number of cyclone events with global warming due to the reduction of baroclinicity. It was also argued that increased levels of atmospheric humidity could lead to increased numbers of intense

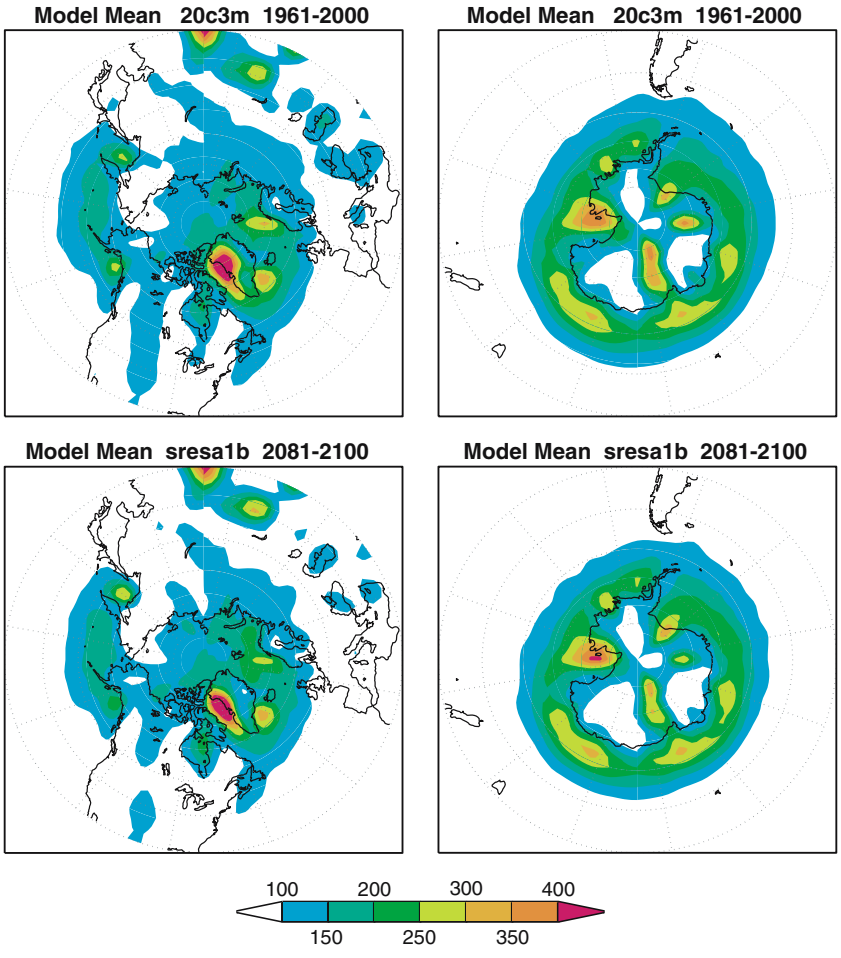


**Fig. 10** The geographical distribution of the model mean for the total number of events. The *upper left panel* displays the number of events for the Northern hemisphere for the period 1961–2000 from the climate of the twentieth century experiment. The *lower left panel* shows the number of events for the period 2081–2100, scaled by a factor of 2, from the SRES A1B experiment for the Northern Hemisphere. The *right panels* displays the corresponding results for the Southern Hemisphere

events. It would be interesting to determine if there is a cause and effect relationship between the reduction of the total events and the increase of intense events. One possible link between the two phenomena is that the increased numbers of intense events will result in elevated levels of poleward heat transport and this will provide increased stability to the atmosphere. This increased stability will be unfavourable for baroclinic development resulting in fewer numbers of cyclones in total. If this is the case, then interannual variability of the total number of events and the interannual variability of the number of intense events will be negatively correlated. The two NCAR models provided several simulations of more than 100 years for which the above correlations were computed after removal of a quadratic trend. The correlations and corresponding $t$ values are given in Table 4. The column labelled length is the number of years in the time series. The table shows that the numbers of total events and intense events are generally significantly negatively correlated, which supports the hypothesis that the numbers of intense events and the number of total events are not independent and suggests that an increase in intense events leads to a decrease in the total number of events.

## 4 Summary

We have examined changes in cyclone events in a variety of experiments using the models participating in an IPCC diagnostic exercise. The modelling groups provided results for three of the IPCC climate change scenarios, SRES B1, SRES A1B, and SRES A2. Since there are two hemispheres, this provided six opportunities to examine changes in the mid-latitude cyclone behaviour in each model. For all the scenarios, all the models simulated a reduction in the total number of cyclone events with the reduction being larger in the Southern Hemisphere than the Northern Hemisphere. For a majority of the experiments, the models simulated an increase in the number of intense events where an intense events is defined as an event with a central pressure of less than 970 mb for the Northern Hemisphere and less than 960 mb for the Southern

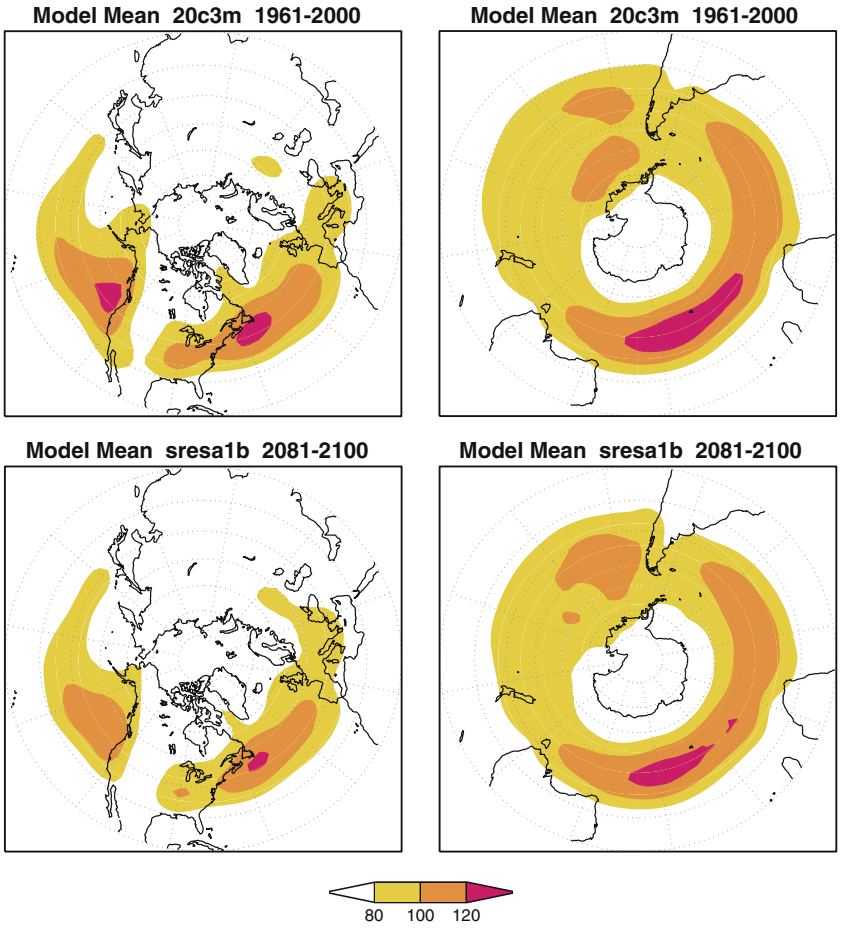


**Fig. 11** Same as Fig. 10 except for the filtered variance of the 500 mb meridional wind ($m^2$ $s^{-2}$)

**Table 4** Correlations between the total number of cyclone events and the number of intense events for long simulations of the pre-industrial control runs and the climate of the twentieth century simulations. The table gives the length of the simulation in years, the correlations, and the corresponding *t* values

| Correlation between total events and intense events | | | | | | | |
|---|---|---|---|---|---|---|---|
| Model | Experiment | Run | Length | Northern Hemisphere | | Southern Hemisphere | |
| | | | | Correlation | *t* Value | Correlation | *t* Value |
| ncar_pcm | Control | 1 | 748 | −0.226 | −6.3 | −0.375 | −11.1 |
| ncar_pcm | Twentieth century | 1 | 110 | −0.469 | −5.5 | −0.425 | −4.9 |
| | | 2 | 110 | −0.511 | −6.1 | −0.328 | −3.6 |
| | | 3 | 110 | −0.307 | −3.3 | −0.172 | −1.8 |
| | | 4 | 110 | −0.279 | −3.0 | −0.497 | −6.0 |
| ncar_ccsm | Control | 1 | 230 | −0.550 | −9.9 | −0.282 | −4.4 |
| | | 2 | 370 | −0.675 | −17.5 | −0.309 | −6.2 |
| ncar_ccsm | Twentieth century | 1 | 130 | −0.444 | −5.6 | −0.244 | −2.8 |
| | | 3 | 130 | −0.506 | −6.6 | −0.303 | −3.6 |
| | | 6 | 130 | −0.622 | −8.9 | −0.340 | −4.1 |

hemisphere. The intense event results are quite 'noisy' as a result of the increased sampling variability resulting from the reduced numbers of intense events. In spite of this variability, the model means for the three scenarios and the two hemisphere exhibit a consistent increase in the number of intense events. Finally, changes in the positions of the simulated storm tracks were investigated by examining changes in the geographical distribution of the total cyclone events and in the distribution of the filtered variance of the meridional wind. These results showed that there is no obvious shift in storm tracks with global warming.

**Acknowledgements** We acknowledge the international modelling groups for providing their data for analysis, the Program for Climate Model Diagnosis and Intercomparison (PCMDI) for collecting and archiving the model data, the JSC/CLIVAR Working

Group on Coupled Modelling (WGCM) and their Coupled Model Intercomparison Project (CMIP) and Climate Simulation Panel for organizing the model data analysis activity, and the IPCC WG1 TSU for technical support. The IPCC Data Archive at Lawrence Livermore National Laboratory is supported by the Office of Science, U.S. Department of Energy. We thank the two referees for their efforts in reviewing the paper.

## References

Bleck R (2002) An oceanic general circulation model framed in hybrid isopycnic-cartesian coordinates. Ocean Model 4:55–88

Boer GJ, McFarlane NA, Lazare M (1992) Greenhouse gas-induced climate change simulated with the CCC second generation general circulation model. J Climate 5:1045–1077

Delworth TL, Broccoli AJ, Rosati A, Stouffer RJ, Balaji V, Beelsey JA, Cooke WF, Dixon KW, Dunne J, Dunne KA, Durachta JW, Findell KL, Ginoux P, Gnanadesikan A, Gordon CT, Griffies SM, Gudgel R, Harrison MJ, Held IM, Hemler RS, Horowitz LW, Klein SA, Knutson TR, Kushner PJ, Langenhorst AR, Lee H-C, Lin S-J, Lu J, Malyshev SL, Milly PCD, Ramaswamy V, Russell J, Schwarzkopf MD, Shevliakova E, Sirutis JJ, Spelman MJ, Stern WF, Winton M, Wittenberg AT, Wyman B, Zeng F, Zhang R (2005) GFDL's CM2 global coupled climate models. Part I: formulation and simulation characteristics. J Climate (in press)

Diansky NA, Volodin EM (2002) Simulation of present day climate with a coupled atmosphere–ocean general circulation model. Izv Atmos Ocean Phys (English Translation) 36(6):732–747

Gnanadesikan A, Griffies SM, Dixon K, Balaji V, Barreiro M, Beesley JA, Cooke W, Delworth T, Dunne JP, Gerdes R, Harrison MJ, Held I, Hurlin WJ, Lee HC, Liang Z, Nong G, Pacanowski RC, Rosati A, Russell J, Samuels BL, Spelman M, Sweeney C, Stouffer RJ, Vecchi G, Winton M, Wittenberg A, Zeg F, Zhang R (2005) GFDL's CM2 global coupled climate models. Part II: the baseline ocean simulation. J Climate (in press)

Houghton JT, Ding Y, Griggs DJ, Noguer M, Van der Linden PJ, Dai X, Maskell K, Johnson CA (eds) (2001) Climate change 2001, the scientific basis. Cambridge University Press, London

Lambert SJ (1995) The effect of enhanced greenhouse warming on winter cyclone frequencies and strengths. J Climate 8:1447–1452

Lambert SJ (2004) Changes in winter cyclone frequencies and strengths in transient enhanced greenhouse warming simulations using two coupled climate models. Atmos Ocean 42:173–181

Lambert SJ, Sheng J, Boyle JS (2002) Winter cyclone frequencies in thirteen models participating in the Atmospheric Model Intercomparison Project (AMIP1). Climate Dynam 19:1–16

Marsland SJ, Haak H, Jungclaus JH, Latif M, Roske F (2003) The Max Planck Institute global ocean/sea-ice model with orthogonal curvilinear coordinates. Ocean Model 5:91–127

Petterssen S (1956) Weather analysis and forecasting, vol 1. McGraw-Hill, New York, 422 pp

Roechner E, Bauml G, Bonaventura L, Brokopf R, Esch M, Giorgetta M, Hagemann S, Kirchner I, Kornblueh L, Manzini E, Rhodin A, Schlese U, Schulzweida U, Tompkins A (2003) The atmospheric general circulation model ECHAM5. Part I: model description. Max Planck Institute for Meteorology, Rep. 349, 127 pp (Available from MPI for Meteorology, Bundesstr. 53, Hamburg, Germany)

Russell GL, Miller JR, Rind D (1995) A coupled atmosphere-ocean model for transient climate change studies. Atmos Ocean 33:683–730

Russell GL, Miller JR, Rind D, Ruedy RA, Schmidt GA, Sheth S (2000) Comparison of model and observed regional temperature changes during the past 40 years. J Geophys Res 105:14891–14898

Schmidt GA, Ruedy R, Hansen JE, Aleinov I, Bell N, Bauer M, Bauer S, Cairns B, Canuto V, Cheng Y, Del Gerio A, Faluvegi G, Friend AD, Hall TM, Hu Y, Kelley M, Kiang NY, Koch D, Lacis AA, Lerner J, Lo KK, Miller RL, Nazarenko L, Onas V, Perlwitz J, Perlwitz J, Rind D, Romanou A, Russell GL, Sato M, Shindell D, Stone PH, Sun S, Tausnev N, Thresher D, Yao M-S (2005) Present day atmospheric simulations using GISS Model E: comparison to in-situ satellite and reanalysis data. J Climate (in press)

Sutcliffe RC, Forsdyke AG (1950) The theory and use of upper air thickness patterns in forecasting. Q J R Meteor Soc 76:189–217

Washington WM, Weatherly JW, Meehl GA, Semtner AJ, Bettge TW, Craig AP, Strand WG, Arblaster J, Wayland VB, James R, Zhang Y (2000) Parallel climate model (PCM) control and transient simulations. Climate Dynam 16:755–774

Yukimoto SA, Noda A, Kitoh A, Sugi M, Kitamura Y, Hosaka M, Shibata K, Maeda S, Uchiyama T (2001) The new Meteorological Research Institute coupled GCM (MRI-CGCM2). Pap Meteor Geophys 51:47–88